New Roll-to-Roll Processable PEDOT-Based Polymer with Colorless Bleached State for Flexible Electrochromic Devices

Sven Macher, Marco Schott, Mauro Sassi, Irene Facchinetti, Riccardo Ruffo, Giorgio Patriarca, Luca Beverina, Uwe Posset, Guinevere A. Giffin, and Peer Löbmann*

Conjugated electrochromic (EC) polymers for flexible EC devices (ECDs) generally lack a fully colorless bleached state. A strategy to overcome this drawback is the implementation of a new sidechain-modified poly(3,4-ethylene dioxythiophene) derivative that can be deposited in thin-film form in a customized high-throughput and large-area roll-to-roll polymerization process. The sidechain modification provides enhanced EC properties in terms of visible light transmittance change, $\Delta\tau_v = 59\%$ ($\Delta L^* = 54.1$), contrast ratio (CR = 15.8), coloration efficiency ($\eta = 530$ cm^2 C^{-1}), and color neutrality ($L^* = 83.8$, $a^* = -4.3$, $b^* = -4.1$) in the bleached state. The intense blue-colored polymer thin films exhibit high cycle stability (10 000 cycles) and fast response times. The design, synthesis, and polymerization of the modified 3,4-ethylene dioxythiophene derivative are discussed along with a detailed optical, electrochemical, and spectroelectrochemical characterization of the resulting EC thin films. Finally, a flexible see-through ECD with a visible light transmittance change of $\Delta\tau_v = 47\%$ ($\Delta L^* = 51.9$) and a neutral-colored bleached state is developed.

1. Introduction

Electrochromic (EC) materials, which change their optical properties due to a charge-transfer process,[1–7] are used to design and produce aesthetically pleasing and practical human interfaces. Thus, EC materials can be introduced to smart consumer goods and environments in the fields of architecture, vehicles, interior design, lifestyle and sports. In particular, flexible EC

S. Macher, Dr. M. Schott, Dr. U. Posset, Dr. G. A. Giffin, Prof. P. Löbmann
Fraunhofer Institute for Silicate Research ISC
Fraunhofer R&D Center Electromobility
Neunerplatz 2, D-97082 Würzburg, Germany
E-mail: marco.schott@isc.fraunhofer.de
Dr. M. Sassi, I. Facchinetti, Prof. R. Ruffo, G. Patriarca, Prof. L. Beverina
Department of Materials Science
University of Milano-Bicocca
Via R. Cozzi 55, I-20125 Milano, Italy

The ORCID identification number(s) for the author(s) of this article can be found under https://doi.org/10.1002/adfm.201906254.

devices (ECDs), as non-light emitting, low weight and low power interactive graphics, dynamic shading and display solutions for an intelligent environment, contribute to this trend. Conjugated polymers are one of the main classes of materials that exhibit EC properties as thin films.[3,8–11] Conjugated EC polymers (ECPs), such as poly(3,4-ethylene dioxythiophene) (PEDOT), are generally compatible with high-throughput processes, e.g., roll-to-roll (R2R) deposition. ECPs, therefore, are a large-scale and low-cost solution for ECDs since they can be coated on flexible plastic substrates by means of wet chemical approaches.[12–17] Furthermore, ECPs feature a wide range of vivid colors, response times in the range of seconds, and light transmittance change over 60%. These outstanding EC properties result from an extended conjugated π-electron system. The bandgap between the highest occupied π-electron band and the lowest unoccupied band determines the EC properties like color and color change. Therefore, most ECPs are tunable by tailoring the structure through synthetic modification, which provides the opportunity to diversify and control the redox behavior or the processing of the ECPs.[3,6,11,18–23]

A drawback of most ECPs is the lack of a highly transmissive and fully colorless bleached state. This is the result of a common feature of most donor–acceptor polymers, i.e., the extended tailing of the polaronic and bipolaronic absorption bands into the visible region of the electromagnetic spectrum.[14,24] The residual coloration only becomes acceptable in the case of very thin films, but this comes at the expense of sufficient darkening in the colored state. Most of the literature dedicated to ECPs focuses on the development of materials providing a neutrally colored dark state.[25,26] Although there are a few examples of ECPs fulfilling the demanding color requirements, these materials do not have a completely colorless and highly transmissive bleached state and are incompatible with high-throughput deposition techniques.[3,6,7,27–34] Other materials, such as multichromophoric polymers, can actually offer suitable bleached and colored states, but require elaborate synthesis routes and have an electrochemical operating window, which poses serious stability problems.[18,24] To date, the best EC material in terms of synthetic simplicity, color neutrality

**ADVANCED
SCIENCE NEWS**
www.advancedsciencenews.com

**ADVANCED
FUNCTIONAL
MATERIALS**
www.afm-journal.de

in the bleached state, light transmittance change, and compatibility with high-throughput deposition techniques remains a poly(3,4-propylene dioxythiophene) (ProDOT) derivative. This functionalized ProDOT possesses excellent film-forming properties and a high light transmittance change, but it is still distinctively bluish in the bleached state.[29,35,36]

Strategies presented in the literature to improve color neutrality in the bleached state show that a reduction of the absorption in the visible region of the electromagnetic spectrum can be achieved through a bathochromic shift of the polaronic and bipolaronic bands.[29,35,36] A bathochromic shift in PEDOT-like structures is obtained by the introduction of bulky lateral sidechains that increase the van-der-Waals volume of the polymer and improve the planarity of the conjugated system.[37,38] ProDOT derivatives generally have superior properties as compared to functionalized PEDOT as the sidechains in ProDOT derivatives extend perpendicular to the conjugation plane.[29,35,36] However, a polymer with a seven-membered ring, i.e., ProDOT, is sterically bulkier than the six-membered ring of PEDOT and thus perturbs the S-O interactions ensuring planarity. The introduction of a terminal double bond at the end of the lateral hexyl side chain in the case of poly(3-hexylthiophene) promotes a more pronounced π-stacking between neighboring conjugated polymer chains, which leads to a narrowing of the band gap. Furthermore, the literature demonstrates that the terminal double bond of the lateral hexenyl side chain improves the planarity of the conjugated system and favors intramolecular interactions.[39,40]

Based on this knowledge, a series of 3,4-ethylene dioxythiophene (EDOT) derivatives with a terminal double bond in the lateral sidechain, produced via straightforward synthetic modifications of the EDOT-MeOH precursor, is described herein. All of the EDOT derivatives are electrochemically polymerized and characterized with (in situ) spectroelectrochemistry. The results highlight the dramatic influence of the terminal double bond on the improved light transmittance change and the color neutrality in the bleached state. Furthermore, the best performing compound, which contains a hexenyl sidechain, is scaled-up by changing the deposition technique from an electrochemical to a chemical in situ polymerization (ISP) process on a large R2R scale in an industrially relevant environment.

2. Results and Discussion

All monomers reported in **Figure 1** can be prepared in a straightforward, one-step synthesis starting from the 9:1 mixture of the EDOT-MeOH and ProDOT-OH monomers. This reaction mixture is generally not further purified and employed directly in subsequent elaborations as the removal of the ProDOT minor component does not significantly influence the final properties of the polymerized materials. In the following discussion, the minor isomer ProDOT-OH is omitted for simplicity. The EDOT-EthC3 monomer was prepared, as shown in **Figure 2**, via a Williamson etherification of EDOT-MeOH in anhydrous acetonitrile with allyl bromide in the presence of sodium hydride as the base (50% yield). In a similar manner, EDOT-EthC6 was prepared using 6-bromo-1-hexene as the alkylating agent (42% yield). The scaled-up synthesis of EDOT-EthC6 was carried out in toluene instead of
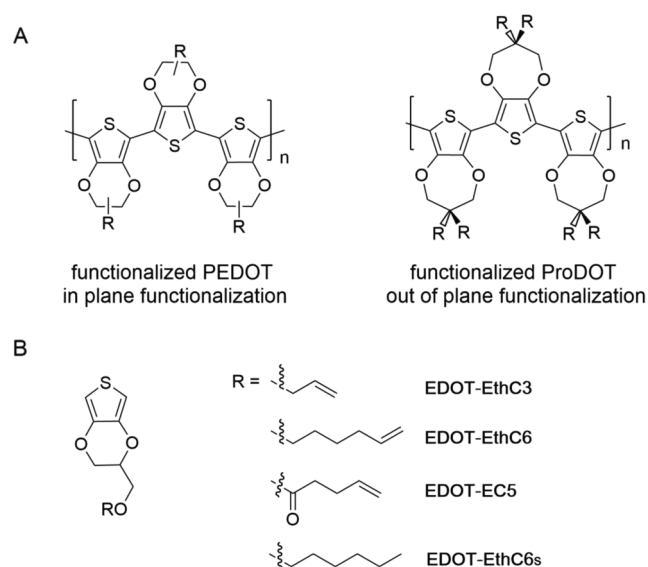

Figure 1. Illustration of the sidechain functionalization of the PEDOT and ProDOT monomers. A) Substitution pattern of PEDOT and ProDOT highlighting the in-plane and out-of-plane geometries. B) Sidechain-functionalized EDOT derivatives bearing a terminal double bond in the lateral solubilizing chain, along with the control derivative EDOT-EthC6s.

acetonitrile and on a 99:1 EDOT-MeOH/ProDOT-OH mixture. EDOT-EC5 was prepared by the Schotten–Baumann esterification of 4-pentenoyl chloride and EDOT-MeOH in refluxing dichloromethane (70% yield). Finally, EDOT-Eth6s was prepared through a phase transfer etherification of EDOT-MeOH
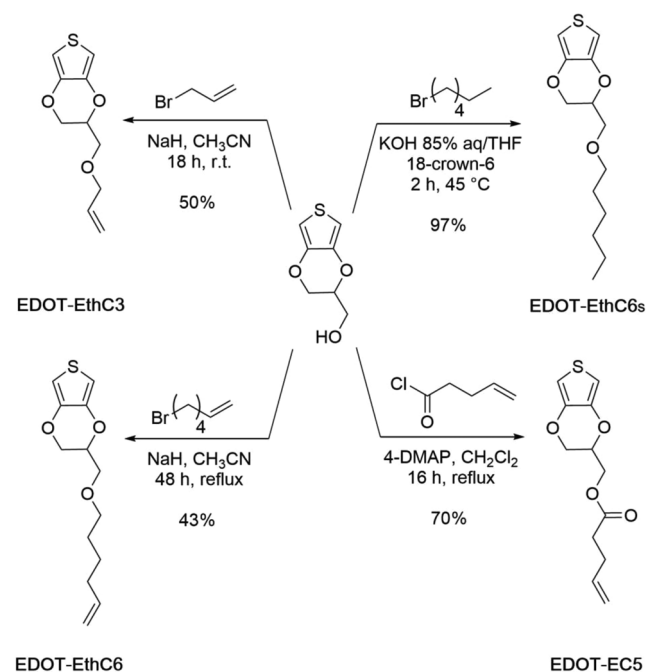

Figure 2. Structural formula of the EDOT derivatives. The standard EDOT:ProDOT derivative isomeric ratio is 9:1, determined by Gas chromatography/mass spectrometry measurements. Reaction protocol to access substituted EDOT derivatives bearing a terminal double bond in the lateral chain and the control derivative EDOT-EthC6s without a terminal double bond.
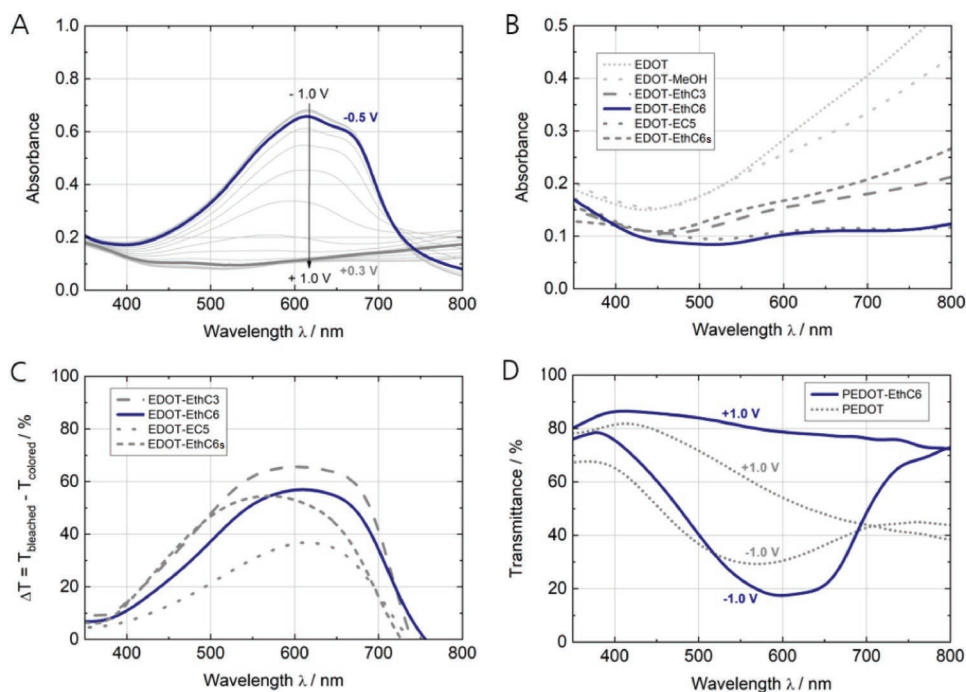
Figure 3. Characterization of the PEDOT-based polymer thin films obtained from the electropolymerization process. A) Absorption spectra at different potentials (1.0 V ↔ −1.0 V vs Ag/AgCl, 0.1 V steps) in steady-state polarization of a PEDOT-EthC6 thin film. B) Absorption spectra of all electropolymerized polymer thin films, a pristine PEDOT thin film, and the precursor PEDOT-MeOH thin film in their corresponding bleached (charged/oxidized) states. C) Transmittance change (ΔT) of all electropolymerized polymer thin films. D) Transmission spectra of chemically (in situ) polymerized PEDOT and PEDOT-EthC6 thin films in their limiting states (bleached (charged/oxidized) at 1.0 V and colored (uncharged/reduced) at −1.0 V).

with 1-bromohexane in tetrahydrofuran/85 wt% potassium hydroxide in the presence of 18-crown-6 as the phase transfer catalyst. The complete experimental procedures as well as the characterization of all new compounds are reported in the Supporting Information (Figures S1–S6, Supporting Information).

All monomers were electrochemically polymerized to EC polymer thin films with comparable film thickness in order to compare the properties of the corresponding polymers on a laboratory scale under standard conditions. **Figure 3**A shows the (in situ) spectroelectrochemical characterization of PEDOT-EthC6, as an example. The absorption spectra illustrate that the PEDOT-EthC6 thin film is in its highly transmissive (bleached) state at a potential above 1.0 V versus Ag/AgCl, where the PEDOT-derived backbone is charged/oxidized and has a very weak absorption. At a potential of −1.0 V versus Ag/AgCl, the polymer thin film is in the uncharged/reduced state and the layer turns deep blue due to a strong and broad absorption with a maximum at around 620 nm. The spectroelectrochemical characterization of all the other PEDOT derivatives can be found in the Supporting Information (Figures S1–S6, Supporting Information). Figure 3B shows the comparison between the absorption spectra of all polymers in the bleached state and the corresponding absorptions of PEDOT-MeOH—the common precursor—and the unsubstituted PEDOT. The shift of the polaronic/bipolaronic band toward the near-infrared region is particularly evident for PEDOT-EthC6 and PEDOT-EC5, the monomers containing longer alkyl side chains with a terminal double bond, which yields a less-colored bleached state.[37–40] Figure 3C shows that PEDOT-EthC3 and PEDOT-

EthC6 have the highest light transmittance change (ΔT) of the series. However, while PEDOT-EthC3 is not colorless in its bleached state, PEDOT-EthC6 has a virtually colorless bleached state and a high light transmittance change, which made it the polymer of choice for upscaling.

A technique more suitable for upscaling is a chemical ISP process, since it is compatible with high-throughput and large-area R2R deposition methods. Therefore, all monomers were also chemically polymerized according to literature protocols.[41] Only the EDOT-EthC6 derivative gave results comparable with those obtained by electrochemical polymerization. Figure 3D shows a direct comparison between the limiting states in the spectroelectrochemistry of chemically (in situ) polymerized PEDOT and PEDOT-EthC6. Both the increase in the bleached state transmittance and the light transmittance change are evident for PEDOT-EthC6.

For upscaling, a modular R2R coating machine, shown in **Figure 4**A, was developed and customized to suit the unique ISP process. The polymerization of the EDOT-EthC6 occurs after deposition of a polymerization mixture—in situ—on the PET-ITO (Indium tin oxide coated polyethylene terephthalate) film. The polymerization mixture contains the EDOT-EthC6 monomer, dissolved in *n*-butanol, iron (III)-tosylate as the oxidizing agent and *n*-propyl amine as the moderator. The PET-ITO substrate was coated using a slot die with a maximum coating width of 500 mm (Figure 4B). The film thickness was adjusted by varying the web speed (ranging from 0.5 to 1.0 m min⁻¹) and the delivery volume (ranging from 3.0 to 4.0 mL min⁻¹). The polymerization of the EDOT-EthC6 takes place in a 6 m

**ADVANCED
SCIENCE NEWS**
www.advancedsciencenews.com
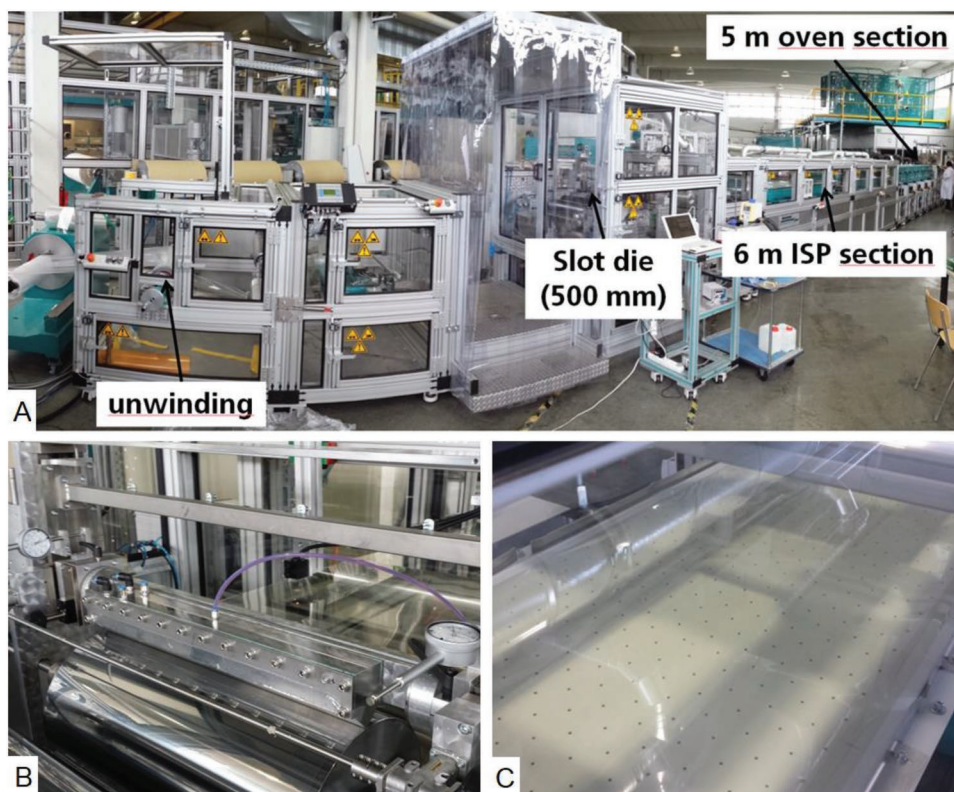
**ADVANCED
FUNCTIONAL
MATERIALS**
www.afm-journal.de

Figure 4. Large-scale deposition of PEDOT-EthC6 thin films on PET-ITO. A) Modular R2R coating machine with unwinding unit, slot die, ISP, and oven section. B) Slot die deposition. C) ISP section (6 m), showing a yellowish colored wet film.

polymerization section, shown in Figure 4C. After a drying step (5 m oven section at 120 °C), the PEDOT-EthC6 films were rewound and stored. In a second R2R process, the PEDOT-EthC6 thin films were rinsed in reservoirs successively filled with *n*-butanol, *n*-butanol–water mixtures, and ethanol and subsequently dried in a 1 m oven module at 100 °C. The web speed was set to 0.2 m min^{-1}. The rinsed PEDOT-EthC6 thin films are partly oxidized ("as obtained") and thus show a grayish, but transparent tint. In **Figure 5**A, a scanning electron microscopy (SEM) image of a PEDOT-EthC6 thin film is depicted. The topography of the PEDOT-EthC6 layer appears as a characteristic 3D, periodical honeycomb pattern. The honeycomb structure is ascribed to the rinsing process of the solid

PEDOT-EthC6 thin films, in which the remaining oxidizing agent is removed from the polymer film with the alcohol and water solvents. It is expected that the increased surface area and structuring of the layer accelerates the anion insertion process during the color change of the EC thin film. The cross-section image in Figure 5B demonstrates a film thickness of around 400 nm and a smooth interface between the PEDOT-EthC6 and ITO layer, thus indicating good interlayer adhesion and a highly transparent film stack. The high transparency is reflected in the haze measurement with values below 1%, which means that only very little light is scattered at a wide angle or diffused due to macroscopic irregularities or rough interfaces in the EC polymer thin film. A change in the electronic structure of
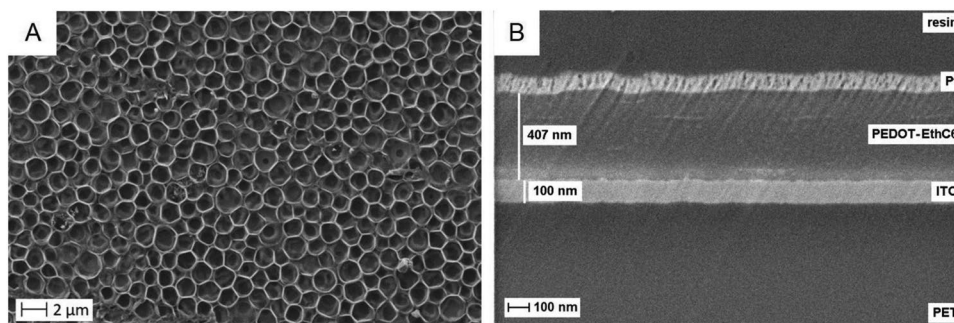

Figure 5. Characteristic SEM images of a PEDOT-EthC6 thin film. A) Surface morphology, showing a characteristic 3D, periodical honeycomb pattern. B) Cross-section image of a PEDOT-EthC6 layer on PET-ITO indicating a film thickness of around 400 nm.
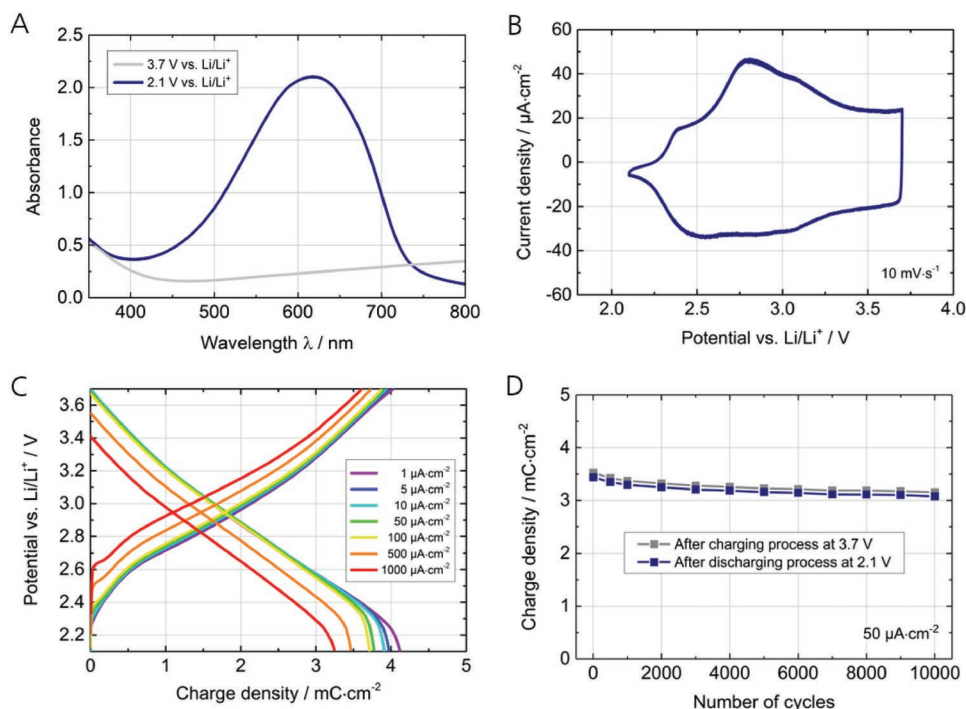
Figure 6. Spectroelectrochemical and electrochemical characterization of the PEDOT-EthC6 thin films on PET-ITO in 1 M LiClO$_4$/PC. A) Absorption spectra of the PEDOT-EthC6 thin film in its charged/oxidized (3.7 V vs Li/Li$^+$) and uncharged/reduced (2.1 V vs Li/Li$^+$) state. B) Cyclic voltammogram at a scan rate of 10 mV s^{-1}. C) Charging/discharging behavior at different current densities (from 1 to 1000 μA cm^{-2}). D) Cycle stability measurements over 10 000 switching cycles (2.1 V ↔ 3.7 V vs Li/Li$^+$) at a current density of 50 μA cm^{-2}.

the EC polymer by an externally induced charge transfer process leads to a modification of the transmittance and color of the thin film. However, the microstructure of the polymer thin film is not affected thereby and remains transparent (haze below 1%) in both, the bleached and the dark state. The spectroelectrochemical characterization of ISP-manufactured PEDOT-EthC6 thin films is depicted in **Figure 6**A. The absorption spectra illustrate that the color neutral (bleached) state is reached at a potential above 3.7 V versus Li/Li$^+$. The PEDOT-derived backbone is charged/oxidized and shows a very weak absorption. The visible light transmittance τ_v is 63%. At a potential of 2.1 V versus Li/Li$^+$, a strong and broad absorption with a maximum at around 620 nm (τ_v = 4%) is responsible for the deep blue color (darkened) that occurs when the backbone is in its uncharged/reduced state. The analysis of the $L^*a^*b^*$ values (CIELAB color space), L^* = 83.8, a^* = −4.3, b^* = −4.1 and L^* = 29.7, a^* = 17.0, b^* = −58.2, further confirms the neutral color of the bleached state and the deep blue color of the darkened state, respectively. The visible light transmittance change is $\Delta\tau_v$ = 59% (ΔL^* = 54.1) and the corresponding contrast ratio (CR = $\tau_{v,\,bleached}/\tau_{v,\,colored}$) can be estimated as CR = 15.8. The coloration efficiency (η = log($T_{bleached}/T_{colored}$)/q) at the absorption maximum of 620 nm is calculated to be η = 530 cm^2 C^{-1}, which substantially exceeds most commonly used inorganic EC materials.[11,24] The ISP-manufactured PEDOT-EthC6 film is significantly thicker than the electrochemically polymerized PEDOT-EthC6 thin films, which leads to a higher CR. The visible light transmittance change $\Delta\tau_v$ is not affected. The appropriate film thickness depends on the application and can be adjusted by the web speed and the

delivery volume of the polymerization mixture during the ISP process.

The electrochemical properties of the ISP-manufactured PEDOT-EthC6 thin films were initially investigated by cyclic voltammetry (CV). Figure 6B shows the CVs at a scan rate of 10 mV s^{-1}. The ISP film exhibits reversible redox peaks at a potential of 2.8 V (cathodic scan) and 2.5 V (anodic scan) versus Li/Li$^+$ (ΔE_p = 300 mV) corresponding to the oxidation (bleaching) and reduction (coloring) process, respectively, of the conjugated backbone. The substantially broadened cathodic and anodic half-waves are an unavoidable consequence of hindered diffusion and insertion of the perchlorate counter anions and molecular inhomogeneities in the polymer matrix (e.g., different chain length, different sizes of crystalline domains, polymer particle dimensions, pore dimensions). The mentioned inhomogeneities are assigned to the molecular level and therefore affect the redox potentials, but do not cause haze. The coulombic efficiency is approximately 1, indicating a reversible redox process. The results from the CV measurements are in agreement with previously published data of similar PEDOT and PEDOT-like species.[8,19,41] The PEDOT-EthC6 films were further characterized in galvanostatic charging/discharging experiments with current densities between 1 and 1000 μA cm^{-2}. The charge/discharge curves are depicted in Figure 6C. They also show a reversible oxidation and reduction behavior, while the Coulombic efficiency is around 98% at a current density of 50 μA cm^{-2}. The maximum charge density is determined after the discharge (reduction) process at 2.1 V versus Li/Li$^+$ and depends on the applied current density. The PEDOT-EthC6 film exhibits a maximum charge density of 4.1 mC cm^{-2} at a current

1906254 (5 of 8)

ADVANCED
SCIENCE NEWS
www.advancedsciencenews.com

ADVANCED
FUNCTIONAL
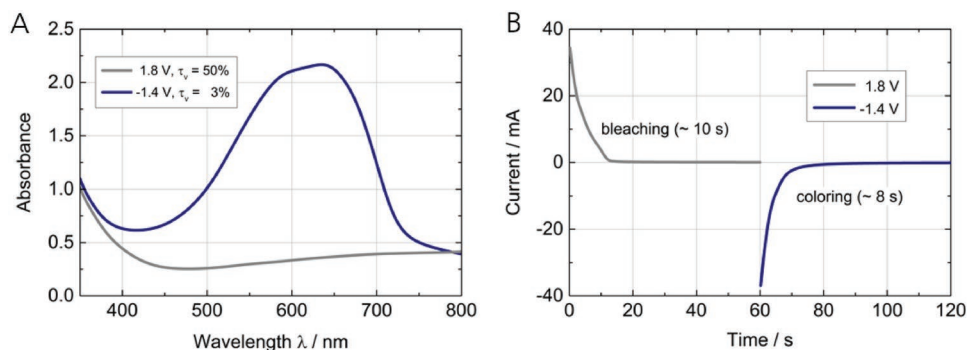**MATERIALS**
www.afm-journal.de

Figure 7. Characterization of the full ECD with PEDOT-EthC6 as the working electrode and PB as the counter electrode with a LiClO$_4$-containing polymer electrolyte. A) Absorption spectra of the full device with $\Delta\tau_v$ = 47% (3% ↔ 50%) and ΔL^* = 51.9. B) Response time measurement during potentiostatic cycling (60 s at 1.8 V ↔ 60 s at −1.4 V) with a response time of around 10 s for the bleaching process and 8 s for the coloring process.

density of 1 μA cm^{-2}. The results from the cycle stability measurements are shown in Figure 6D. The measurement was performed by charging and discharging the PEDOT-EthC6 thin film on PET-ITO in a 1 M LiClO$_4$/PC electrolyte with a current density of 50 μA cm^{-2}. The results indicate a reversible redox switching behavior with only a small drop of charge density in the first 1000 cycles (0.1 mC cm^{-2}), which can be attributed to the formation processes and further electrochemical polymerization of the polymer chain. Additional loss of charge density can be explained by hindered diffusion and insertion of the perchlorate counter anions during the fast charge/discharge experiment. After 10 000 switching cycles, the PEDOT-EthC6 thin film on PET-ITO shows a total charge retention of more than 91%, the charge density decreases from 3.5 to 3.2 mC cm^{-2}. In situ spectroelectrochemical characterization before and after the cycle stability measurements is depicted in Figure S7 in the Supporting Information.

The performance of the PEDOT-EthC6 thin films was tested under inert conditions in a typical sandwich-like ECD with an active area of 5 × 5 cm². The cathodically coloring PEDOT-EthC6 functions as the working electrode, while a Prussian blue (PB) thin film on PET-ITO was used as the anodically coloring, and therefore complementarily switching, counter electrode.[42–44] The colored state (−1.4 V) shows an intense deep blue color (L^* = 24.4, a^* = 10.4, b^* = −47.2), whereas the bleached state (1.8 V) is distinguished by a highly transmissive neutral coloration (L^* = 76.3, a^* = −5.7, b^* = −2.5). The high transparency of the ECD is reflected in the haze measurement with values below 2% for the colored and bleached state. It should be noted that the optical properties of the PET-ITO substrate are included as the measurements were conducted versus air. The corresponding absorption spectra of the colored and bleached state are presented in **Figure 7**A. In the dark state, a strong and broad absorption peak with a maximum at 635 nm is visible, which is attributed to the signal of the PEDOT-EthC6 film superimposed with that of the PB thin film. The shoulder at around 690 nm is associated with the PB layer, which on its own exhibits an absorption maximum at 690 nm. The visible light transmittance change $\Delta\tau_v$ can be calculated as 47% (ΔL^* = 51.9) and the contrast ratio CR is estimated to be 16.7, a result which clearly outperforms the properties of commonly used PEDOT-based ECD.[9] Furthermore, the response time, which is considered to be the time corresponding to a current

drop to 10% of the starting (maximum) value, was analyzed in a potentiostatic experiment (Figure 7B). For the bleaching and coloring processes, a response time of around 8 and 10 s, respectively, was measured. The response time of the full device (PEDOT-EthC6/PB) is limited by the sheet resistance of the PET-ITO (approx. 50 Ω sq.$^{-1}$) and the insulating PB layer. The cycling stability of the ECD (100 cycles) is shown in Figure S9 in the Supporting Information, where the enhanced durability is demonstrated with a total charge retention of more than 97%.

3. Conclusion

Sidechain-modified EDOT derivatives, especially the EDOT-EthC6 compound, can be accessed by a simple and straightforward synthesis. The EC film production can be scaled-up to the pilot-line scale via a customized large-area and high-throughput R2R process. The PEDOT-EthC6 thin films, obtained from the R2R process, have enhanced EC properties in terms of coloration efficiency, transmittance, and color neutrality in the bleached state, cycle stability, and reversibility. The detailed characterization of the up-scaled ECP demonstrates that the incorporation of a sidechain with a terminal double bond yields a material with a performance that surpasses any other PEDOT-related material described in the literature. The PEDOT-EthC6 films were further successfully incorporated into a proof-of-concept complementary-switching ECD (PEDOT-EthC6 vs PB). The unique characteristics of PEDOT-EthC6 combined with the simple and scalable synthesis of the monomer results in a rare material that meets high requirements for R2R processable ECP.

4. Experimental Section

without further purification unless otherwise noted. All monomers were electrochemically polymerized in order to compare the properties of the corresponding polymers under standard conditions. The electropolymerization was performed using a potentiostat/galvanostat PARSTAT 2273 from Princeton Applied Research, by means of CV, chronoamperometry, and chronopotentiometry techniques in a nitrogen-filled glove box. The electrodeposition was performed in a three-electrode cell with fluorine-doped tin oxide glass (15 Ω sq.$^{-1}$, 1 cm^2) as the working electrode, platinum as the counter electrode, and a Ag/AgCl wire as pseudo-reference. The 5×10^{-3} M monomer solutions in the supporting electrolyte, 0.1 M tetrabutylammonium perchlorate (TBAClO$_4$) in anhydrous propylene carbonate (PC), were used. The pseudo-reference electrode was calibrated before and after each measurement using a 5×10^{-3} M solution of ferrocene in the electrolyte. For the manufacturing of the PEDOT-EthC6 layers, the polymerization mixture was prepared as previously described. ECDs (active area: 5×5 cm^2) were assembled in a sandwich-like configuration with the R2R-produced PEDOT-EthC6 on PET-ITO as working electrode and PB on PET-ITO as counter electrode. A proprietary methyl acrylate/ethyl methacrylate-copolymer-based electrolyte, swollen with a solvent mixture of PC and diethyl carbonate (DEC) containing 1 M LiClO$_4$ was used. The amount of light that is diffused or scattered by the EC polymer thin films (haze) was measured with a Hazegard XL-211 hazemeter from Pacific Scientific with air as a reference. Transparency is understood in this case as the physical property of a material to allow light passing through the material without being scattered, whereas transmittance is considered to be the ratio of transmitted to incident light and refers to an energy loss by absorption, scattering or reflection. The R2R-prepared PEDOT-EthC6 thin films were investigated with a field emission SEM Ultra 55 from Carl Zeiss. The appropriate parameters were given with the corresponding images. A Solartron Multistat 1470E multi-channel potentiostat/galvanostat was used for the electrochemical characterization of the R2R-deposited PEDOT-EthC6 thin films. All measurements were performed under argon atmosphere at room temperature with lithium as counter and reference electrode in a 1 M LiClO$_4$/PC electrolyte. The cycle stability was measured using a galvanostatic charging/discharging measurement procedure for up to 10 000 switching cycles (current density: 50 μA cm^{-2}). Optical, colorimetric (CIELAB color space, with $L*$ (lightness from black to white (0–100)), $a*$ (negative values indicate green, positive values indicate magenta), and $b*$ (negative values indicate blue, positive values indicate yellow)), and spectroelectrochemical characterizations of the R2R-deposited PEDOT-EthC6 thin films were conducted in situ using an Avantes AvaSpec-2048 standard fiber optic spectrometer combined with a balanced deuterium-halogen light source. All measurements were performed under argon atmosphere at room temperature with lithium as counter and reference electrode in a 1 M LiClO$_4$/PC electrolyte. Spectroelectrochemical characterizations of the electrochemically polymerized thin films were conducted in situ using a SEC2000 spectrometer (ALS), using platinum as the counter electrode and a Ag/AgCl wire as pseudo-reference. All measurements were performed in a nitrogen-filled glove box using the potentiostat/galvanostat PARSTAT 2273 (Princeton Applied Research). The pseudo-reference electrode was calibrated before and after each measurement using a 5×10^{-3} M solution of ferrocene in the supporting electrolyte. ECDs with an active area of 5×5 cm^2 were characterized by means of CV analysis and response time. UV-vis spectra were recorded in situ during potentiostatic switching of the device at room temperature under an argon atmosphere.

Supporting Information

Supporting Information is available from the Wiley Online Library or from the author.

Conflict of Interest

The authors declare no conflict of interest.

[1] R. D. Rauh, *Electrochim. Acta* **1999**, *44*, 3165.
[2] W. J. Hee, M. A. Alghoul, B. Bakhtyar, O. Elayeb, M. A. Shameri, M. S. Alrubaih, K. Sopian, *Renewable Sustainable Energy Rev.* **2015**, *42*, 323.
[3] R. J. Mortimer, D. R. Rosseinsky, P. M. S. Monk, *Electrochromic Materials and Devices*, Wiley-VCH, Weinheim, Germany **2015**.
[4] R. Baetens, B. P. Jelle, A. Gustavsen, *Sol. Energy Mater. Sol. Cells* **2010**, *94*, 87.
[5] S. D. Rezaei, S. Shannigrahi, S. Ramakrishna, *Sol. Energy Mater. Sol. Cells* **2017**, *159*, 26.
[6] C. G. Granqvist, M. A. Arvizu, İ. Bayrak Pehlivan, H.-Y. Qu, R.-T. Wen, G. A. Niklasson, *Electrochim. Acta* **2018**, *259*, 1170.
[7] D. R. Rosseinsky, R. J. Mortimer, *Adv. Mater.* **2001**, *13*, 783.
[8] L. Groenendaal, G. Zotti, P.-H. Aubert, S. M. Waybright, J. R. Reynolds, *Adv. Mater.* **2003**, *15*, 855.
[9] H. W. Heuer, R. Wehrmann, S. Kirchmeyer, *Adv. Funct. Mater.* **2002**, *12*, 89.
[10] W. T. Neo, Q. Ye, S.-J. Chua, J. Xu, *J. Mater. Chem. C* **2016**, *4*, 7364.
[11] L. Groenendaal, F. Jonas, D. Freitag, H. Pielartzik, J. R. Reynolds, *Adv. Mater.* **2000**, *12*, 481.
[12] A. L.-S. Eh, A. W. M. Tan, X. Cheng, S. Magdassi, P. S. Lee, *Energy Technol.* **2018**, *6*, 33.
[13] C. G. Granqvist, İ. Bayrak Pehlivan, G. A. Niklasson, *Surf. Coat. Technol.* **2018**, *336*, 133.
[14] M. Sassi, M. M. Salamone, R. Ruffo, C. M. Mari, G. A. Pagani, L. Beverina, *Adv. Mater.* **2012**, *24*, 2004.
[15] J. Jensen, F. C. Krebs, *Adv. Mater.* **2014**, *26*, 7231.
[16] J. Jensen, M. Hösel, A. L. Dyer, F. C. Krebs, *Adv. Funct. Mater.* **2015**, *25*, 2073.
[17] H. Wang, M. Barrett, B. Duane, J. Gu, F. Zenhausern, *Mater. Sci. Eng., B* **2018**, *228*, 167.
[18] L. Beverina, G. A. Pagani, M. Sassi, *Chem. Commun.* **2014**, *50*, 5413.
[19] S. Duluard, B. Ouvrard, A. Celik-Cochet, G. Campet, U. Posset, G. Schottner, M.-H. Delville, *J. Phys. Chem. B* **2010**, *114*, 7445.
[20] P. M. Beaujuge, J. R. Reynolds, *Chem. Rev.* **2010**, *110*, 268.
[21] G. P. T. Ganesh, R. Ravi, B. Deb, *Sol. Energy Mater. Sol. Cells* **2015**, *140*, 17.
[22] W. M. Kline, R. G. Lorenzini, G. A. Sotzing, *Color. Technol.* **2014**, *130*, 73.
[23] C. G. Granqvist, E. Avendaño, A. Azens, *Thin Solid Films* **2003**, *442*, 201.

[24] M. Sassi, M. M. Salamone, R. Ruffo, G. E. Patriarca, C. M. Mari, G. A. Pagani, U. Posset, L. Beverina, *Adv. Funct. Mater.* **2016**, *26*, 5240.

[25] F. C. Krebs, *Nat. Mater.* **2008**, *7*, 766.

[26] P. M. Beaujuge, S. Ellinger, J. R. Reynolds, *Nat. Mater.* **2008**, *7*, 795.

[27] A. M. Österholm, D. E. Shen, J. A. Kerszulis, R. H. Bulloch, M. Kuepfert, A. L. Dyer, J. R. Reynolds, *ACS Appl. Mater. Interfaces* **2015**, *7*, 1413.

[28] A. M. Österholm, D. E. Shen, D. S. Gottfried, J. R. Reynolds, *Adv. Mater. Technol.* **2016**, *1*, 1600063.

[29] J. A. Kerszulis, K. E. Johnson, M. Kuepfert, D. Khoshabo, A. L. Dyer, J. R. Reynolds, *J. Mater. Chem. C* **2015**, *3*, 3211.

[30] C. M. Amb, A. L. Dyer, J. R. Reynolds, *Chem. Mater.* **2011**, *23*, 397.

[31] C. M. Lampert, A. Agrawal, C. Baertlien, J. Nagai, *Sol. Energy Mater. Sol. Cells* **1999**, *56*, 449.

[32] R. D. Rauh, F. Wang, J. R. Reynolds, D. L. Meeker, *Electrochim. Acta* **2001**, *46*, 2023.

[33] J. Nagai, G. D. McMeeking, Y. Saitoh, *Sol. Energy Mater. Sol. Cells* **1999**, *56*, 309.

[34] S. Hassab, D. E. Shen, A. M. Österholm, M. Da Rocha, G. Song, Y. Alesanco, A. Viñuales, A. Rougier, J. R. Reynolds, J. Padilla, *Sol. Energy Mater. Sol. Cells* **2018**, *185*, 54.

[35] C. L. Gaupp, D. M. Welsh, J. R. Reynolds, *Macromol. Rapid Commun.* **2002**, *23*, 885.

[36] R. M. Walczak, J. S. Cowart, J. R. Reynolds, *J. Mater. Chem.* **2007**, *17*, 254.

[37] J. Roncali, *Chem. Rev.* **1992**, *92*, 711.

[38] J. Roncali, *Chem. Rev.* **1997**, *97*, 173.

[39] S. Miyanishi, K. Tajima, K. Hashimoto, *Macromolecules* **2009**, *42*, 1610.

[40] D. Bagnis, L. Beverina, H. Huang, F. Silvestri, Y. Yao, H. Yan, G. A. Pagani, T. J. Marks, A. Facchetti, *J. Am. Chem. Soc.* **2010**, *132*, 4074.

[41] R. Ruffo, A. Celik-Cochet, U. Posset, C. M. Mari, G. Schottner, *Sol. Energy Mater. Sol. Cells* **2008**, *92*, 140.

[42] A. Kraft, M. Rottmann, K.-H. Heckner, *Sol. Energy Mater. Sol. Cells* **2006**, *90*, 469.

[43] D. Eric Shen, A. M. Österholm, J. R. Reynolds, *J. Mater. Chem. C* **2015**, *3*, 9715.

[44] A. A. Karyakin, *Electroanalysis* **2001**, *13*, 813.